Spectrally-selective Gold Nanorod Coatings for Window Glass

X Xu[1], TH Gibbons[2], MB Cortie[1]

[1]Institute for Nanoscale Technology, University of Technology Sydney, PO Box 123 Broadway, NSW 2007, Australia

[2]AngloGold Ashanti, PO Box Z 5046, Perth, WA 6831, Australia

Abstract

The unique optical properties of gold nanorods, which exhibit tuneable absorption as a function of their aspect ratio, suggest that they might have potential applications in coatings for solar control on windows. Here we explore the properties of coatings produced by attaching gold nanorods to the surface of glass. Such coatings can attenuate solar radiation effectively, even at very low gold contents, but the figure-of-merit, T_{vis}/T_{sol}, of our experimental coatings was close to unity, indicating that they are not spectrally selective, However, calculations are presented to show how coatings comprised of a blend of rods with aspect ratios of greater than 3 can produce coatings with T_{vis}/T_{sol} of up to at least 1.4. The maximum value possible for perfectly spectrally-selective coating in sunlight is 2.08. Unfortunately, the practical realization of such coatings requires the further development of reliable methods to scale up the production of gold nanorods of longer aspect ratios.

Introduction

Glass is very extensively used in modern architecture, both as a means to bring daylight into buildings, and for aesthetic reasons. Many commercial buildings are completely clad in glass, while even domestic residences have significant areas of window. Unfortunately, normal plate glass is not only a window for visible light but also for the invisible infrared (IR) rays of sunlight. This is generally unwelcome in summer since it contributes significantly to heat load in the interior of the building [1]. The relationship of the solar spectrum to the wavelengths perceived by the human eye is shown in Figure 1. An ideal window would transmit most of the visible wavelengths and block all others.

There are various solutions available to attenuate the transfer of solar heat into a building through windows. These vary from the use at time of construction of glass coated with pyrolytic low-e films, to the subsequent retrofitting of windows with cheap tinting films or even sophisticated multi-layer polymer-backed films produced by vacuum sputtering [2]. Continuous nanoscale films of gold or silver are another of the available 'solar glazing' coating options. Use of gold gives pleasant neutral blue tone to the glass (as seen from inside the building) which seems acceptable to the public. Continuous coatings of gold or silver attenuate IR very effectively, primarily by reflecting it. Unfortunately, such coatings have been hitherto applied by vacuum coating techniques which require expensive capital equipment. Amortization of the costs of purchasing and running such equipment has a dominant effect in the financial equation, with the value of the gold used being only a secondary consideration. Also, there is rising opposition to the use of highly reflective window glass, since it produces glare in the surrounding environment.

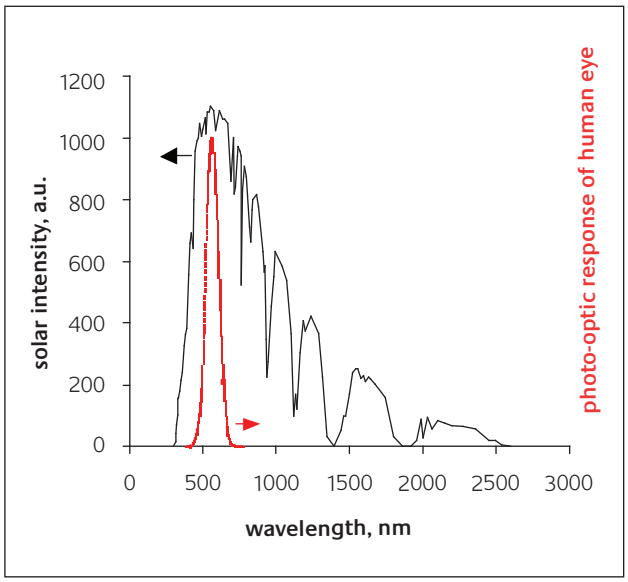

Figure 1

Intensity of solar radiation at various wavelengths, as received on Earth, and the photo-optic response of the human eye

We have previously reported a wet chemical process to deposit nanoscale coatings of gold hemispheres on glass [3], and this seems to have some potential to offer a viable process for the production of tinted glass coatings [4]. The optical properties of our coatings were controlled by the nucleation, growth and coalescence of the gold nano-hemispheres into continuous films [5]. Coatings comprised of well-dispersed gold nanoparticles had only a single surface plasmon absorption peak at about 520 nm, which is in the middle of the visible spectrum and of little use for solar screening. However, when the nanoparticles were relatively close together or even aggregated, they underwent a dipole-dipole interaction with one another which both shifts and broadens the absorption peak to the upper visible and near-IR [6]. Unfortunately, the spectral selectivity between the visible and IR region of these experimental coatings was still inferior when compared to existing solar screening technologies. However, the extensive research recently on gold nanoparticles of more exotic shapes, *e.g.* nanorods [7], nanoshells [8] and 'caps' [9], has inspired us to consider whether these less-symmetrical gold nanoparticles might have applications in solar glazing. Unlike solid nanospheres or hemispheres, these shapes exhibit additional plasmon resonances that depend sensitively on their aspect ratios. Nanorods, for example, not only have a 'transverse' [10] surface plasmon peak at about 520 nm but also manifest another, 'longitudinal', peak at longer wavelengths. The position of this second peak can be shifted from the mid-visible (550 nm) into the infrared (1200 nm) area by increase of the aspect ratio [11], with further adjustment possible by controlling the precise details of shape and symmetry of the rod [12]. In the case of rods it is this second peak that provides the possibility of improved spectral selectivity between the visible and IR regions.

The basic recipe for making rods is now comparatively well understood [7, 13], although there have been no attempts yet, as far as we are aware, to work out how to scale production up to commercially meaningful quantities. In the case of windows the next step after producing the rods is to fix them to the surface of the glass. Attachment of rods to substrates such as mica or glass has already attracted some interest in the recent literature [13], ostensibly because such fixed arrays of nanorods offer a possible means for obtaining the surface enhanced Raman effect (SERS), which is useful in certain types of chemical analysis [14, 15]. There are two possible strategies to achieve this attachment: growing nanorods directly onto the surface, or assembling pre-existing gold nanorods onto the surface.

To achieve the former outcome gold seeds have been attached to a surface functionalized with aminopropyltrimethoxysilane (APTMS) before it was introduced into a rod growth solution [16-18]. With this strategy, neither aggregation of the seed particles nor Ostwald ripening can occur due to the very limited of diffusion of Au in such geometries. Once attached, the nanorods can be imaged and even manipulated by AFM [19]. The disadvantage of this strategy seems to be that only a low density of seeds (1-10 particles/μm^2) are obtained on the surface, which means that the subsequent gold nanorods would not be dense enough to shield the infrared effectively.

Self-assembling of previously produced gold nanorods on glass may currently be the more feasible option [20-23]. In this respect the pH value was found to be one of the most important factors controlling the self assembly process [23, 24]. Variation of pH not only triggered immobilization of gold nanorods but also controlled their density [25] and orientation on the surface [26]. Surface charge is also an important factor. Gold nanorods normally possess a positive charge, but a negative charge can be imparted to them by modification with a polyelectrolyte. The tuning of the surface charge of gold nanorods provides more flexibility for the application of gold nanorods in the immobilization process [27].

In the present paper we describe the results of our research to date on using coatings of gold nanorods on windows for solar screening.

Experimental techniques

Preparation of nanorod suspensions and coatings

HCl, HNO_3, hexadecyltrimethylammoniumbromide (CTAB), γ-amino propyl triethoxy silane (APTES), potassium borohydride (KBH_4), *L*-ascorbic acid and gold were sourced from diverse suppliers. All chemicals were used as-received. Generic soda-lime glass microscope slides were obtained from Livingstone. All H_2O used was purified by double-distillation. $HAuCl_4$ solution was prepared by dissolving pure gold in aqua regia (HCl: HNO_3 3:1 V/V). The surplus amount of HNO_3 was driven by evaporating solution with concentrated HCl. The method may be found elsewhere [3]. It is accepted that some residual HCl content may still be present in the solution.

The gold nanorods were prepared by a modification of the seed-mediated growth method, as originally developed by Nikoobakht [28] and the Murphy group [29]. The 'seed' solution was prepared by mixing 0.10 mL of 0.02 M KBH_4 with 10.0 mL of an aqueous solution containing 0.5 mM $HAuCl_4$ and 0.2 M CTAB. The mixture was vigorously stirred and was used within next 30 minutes. The 'growth' solution was prepared by adding 0.10 mL 0.10 M *L*-ascorbic acid to 10.0 mL aqueous solution containing 0.2 M CTAB, 0.5 mM $HAuCl_4$, and 0.1 mL of 10 mM $AgNO_3$ with stirring. This solution turned from brown-yellow to colourless immediately after mixing. Next, 12 μL of seed solution was added to the growth solution to initiate reaction, which was conducted at room temperature. The reaction can last 30 minutes to a few hours before the colour of the colloid of gold nanorods becomes stable. Large spherical particles could be removed by low speed (2000 rpm) centrifuging.

Finally, 10 mL of colloid was centrifuged at 10,000 rpm for 25 minutes, and the supernatant carefully tipped off. The

pellet was mixed with 10 mL of double-distilled water and the washing procedure was repeated twice to remove surplus CTAB. The final colloid contains 50 – 100 times the concentration of gold nanorods in the original solution with approximately 2 mM of CTAB left. The concentrated gold nanorods colloid was stored in dark conditions, and used over the course of the next several weeks.

Portions of glass slides (30x15mm^2) were cleaned in 50°C of piranha solution ($Vol_{30\%\ H2O2}$: $Vol_{98\%\ H2SO4}$ = 1 : 5) for 30 minutes◇. They were then well rinsed with distilled water and methanol in sequence before use. Thereafter, the slides were dipped into APTES solution (1:5, Vol_{silane} / $Vol_{ethanol}$) for 15 minutes. The coated glass slides were then rinsed with methanol before they were cured in an oven at 110°C for 20 minutes. The silanized glass slides were then dipped into 20 mL of gold nanorods colloid in order to allow the rods to become attached to the silanized surface. (The concentrated gold nanorod colloid was diluted with double-distilled water (1:5) immediately before this step.) The density of the nanorod coating on the glass could be controlled using deposition time, with times of 24 hours giving a high density of coverage.

The coated glass slides were annealed in air at temperatures ranging from ambient to 240°C. The subsequent morphology of the gold nanorods, on carbon or glass substrates, was characterized using a LEO scanning electron microscope (SEM) with in-lens imaging at 2 to 30 kV.

The optical properties of the glass slides were determined using a Cary 5E UV/VIS/IR spectrophotometer, which works in the range of 170 nm to 4300 nm. A resolution of 0.5 nm was used to obtain the visible-IR transmission spectrum of the samples. A scanning rate of 5 nm/s and a spectral bandwidth (SBW) of 2 nm was set during the experiment.

Simulation of optical properties

The optical properties of the gold nanorods were numerically simulated using the FORTRAN code DDSCAT [30], which is based on the discrete-dipole approximation method. The advantage of DDSCAT is that any shape of nano-scaled target can be simulated. It is an approximation method which converts a continuum target into a finite array of polarizable points, which acquire dipole moments in response to the local electric fields [31]. Since, extinction is the result of both absorption and scattering the overall absorption coefficient, α_{ext}, can be expressed as

$$\alpha_{ext} = \eta(C_{abs} + C_{aca}) \qquad (1)$$

where η is the number of particles per unit volume, and C_{abs} and C_{sca} are the absorption and scattering cross-sections respectively.

If multiple scattering is negligible, the irradiance of a beam of light is exponentially attenuated from I_i to I_t in traversing a distance h through a particulate medium:

$$\frac{I_t}{I_i} = \exp(-\alpha_{ext}\, h) \qquad (2)$$

allowing the calculation of optical extinction for a particular particle density [32]. We have used a prolate ellipsoidal spheroid as a physical model to simulate the optical properties of gold nanorods. Such a spheroid can be expressed as [33]:

$$\left(\frac{x}{a}\right)^2 + \left(\frac{y}{b}\right)^2 + \left(\frac{z}{b}\right)^2 = \frac{d^2}{4} \qquad (3)$$

in which a, b are the longitudinal and transverse radii, and d is the interdipole spacing. We define an aspect ratio $\varepsilon = a/b$. The refractive index of the surrounding medium exerts an influence on the calculated spectra but the simulations described here were performed with a simplified medium of refractive index of 1.33, which is the same as that of water. The complex refraction indices of gold and water were obtained from a handbook [34]. Dipole arrays of 25,000 points were applied in the calculations, which was more than sufficient to satisfy the criteria of DDSCAT with respect to numerical stability and accuracy.

Results

Effect of aspect ratio and orientation

The effect that the aspect ratio of the rods have on their optical properties has already been studied by other researchers [7, 13]. In summary, the longitudinal plasmon resonance of the rods can be moved from 520 nm (mid-visible) to over 1200 nm (near-infrared) by increasing the aspect ratio from 1 to 13 respectively [11]. The colour of the rods changes accordingly (Figure 2). Note however that the aspect ratio of the nanorods is not the only reason for their

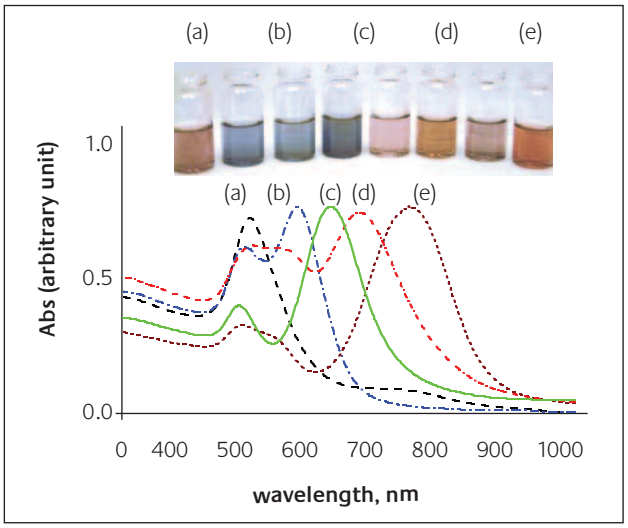

Figure 2

The colour of suspensions of gold nanorods with increasing aspect ratios, as produced by the authors. The colour starts off pink, sweeps through blue and becomes pink again as the position of the longitudinal plasmon resonance moves into the infrared

◇ **Note that piranha solution is very aggressive to skin and that care should be taken when using it.**

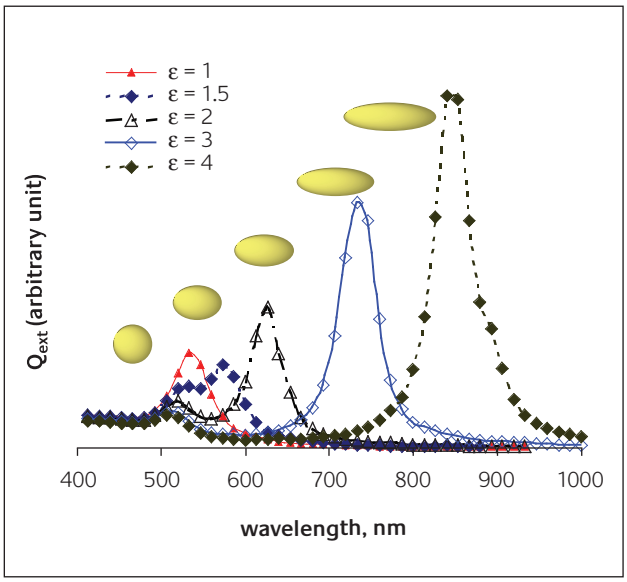

Figure 3

The main factor controlling the position of the longitudinal plasmon resonance is the aspect ratio of the rods. Results shown were calculated for ellipsoidal rods in water

colour. The morphology, volume and packing configuration of the nanorods also contributes to their optical properties, even if their aspect ratios are constant [12, 35, 36]. However, aspect ratio was taken as the only factor in this study to simplify the problem. An illustration of this phenomenon is provided in Figure 3, in which the calculated optical extinction efficiencies of gold rods of various aspect ratios but equal volumes is shown. The surrounding medium in this case is water.

The optical extinction of gold nanorods is also influenced by their orientation with respect to the light, or, more exactly, their orientation with respect to the electric field vector **e** of the light. When the rods are parallel to unpolarized incident radiation, the **e** of the light must necessarily be directed across the transverse directions of the rod. This will lead to only the weaker transverse plasmon resonance at ~520 nm being excited (Figure 4). However, the longitudinal and transverse resonances will both be excited in the case when the rods lie orthogonal to the incident light. The additional excitation of the longitudinal plasmon in this case causes a significant increase in optical extinction (Figure 4).

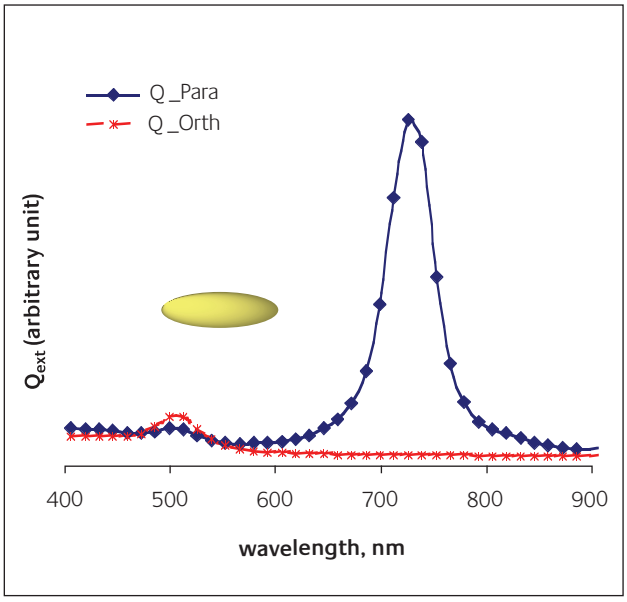

Figure 4

Surface plasmon of gold nanorod with polarized radiation. The terms 'parallel' and 'orthogonal' refer to the orientation of the electric field vector with respect to the long axis of the rod

Attachment of rods to glass

A sample of the nanorods as deposited onto a carbon stub is shown in Figure 5(a). The particles are between 20 and 40 nm long with typical aspect ratios in the range 1.5 to 2. An image of the nanorods immobilized on glass is shown in Figure 5(b). It is puzzling that the particles in this case seem to have a quite different morphology. In particular, they look flatter and more spherical than those on the carbon stub. The reason for this apparent change in morphology on being attached to the glass is not yet known. In any event, the gold nanorods in low density coatings were mostly isolated as deposited, with their longitudinal axes being randomly orientated in the plane of the glass surface.

The optical absorption spectra of glass with a low density coating of gold nanorods and that of the source nanorods in colloidal suspension are given in Figure 6. The two spectra are identical once appropriate adjustments have been made

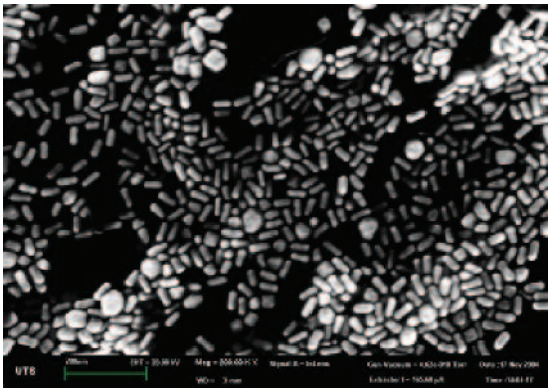

(a) in colloid

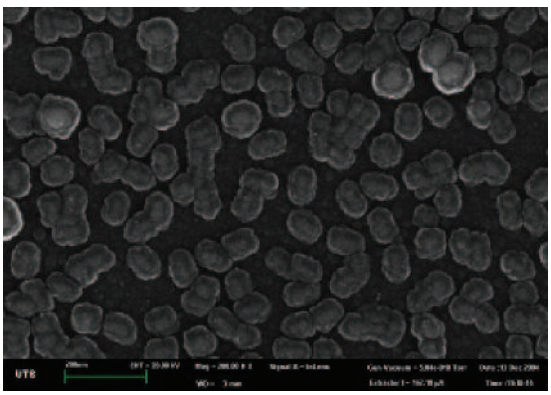

(b) as attached to glass substrate

Figure 5

Morphology of gold nanorods, (green scale bars in images indicate 200 nm)

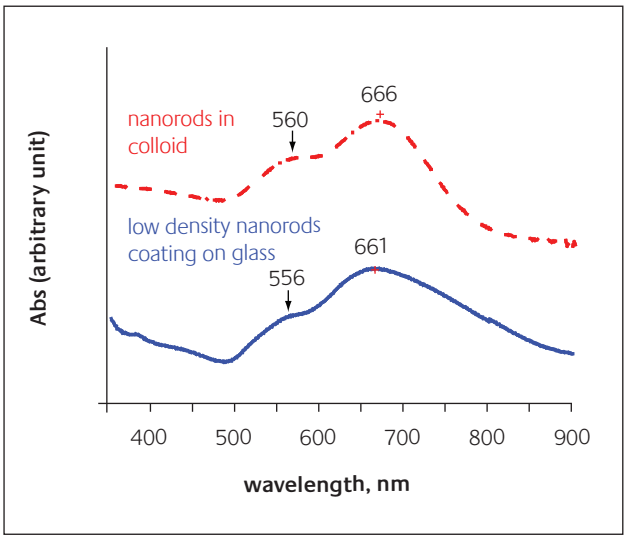

Figure 6
Spectra of colloidal suspension of gold nanorods and of a low density coating of gold nanorods immobilized on glass

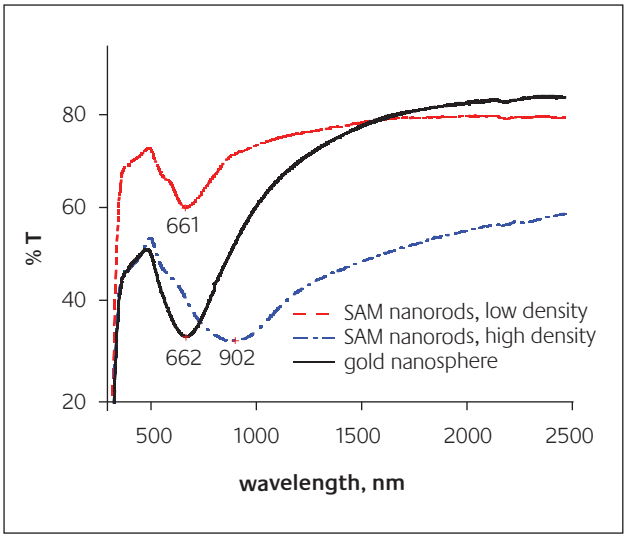

Figure 7
Transmittance spectra of gold nanorods and gold nanosphere coatings

to account for optical density. Apparently, in this case the coating of gold nanorods inherits the optical properties of the colloidal suspension.

A typical transmission spectra of a coating with high packing density is compared in Figure 7 to those of the coating of low packing density, and to an example of a coating comprised of gold nano-hemispheres (the latter was produced in work that has been previously described elsewhere [3, 4]). The three kinds of coatings display quite different optical properties. The coating of low packing density showed a similar transmittance in the near-infrared to the coating of nano-hemispheres, but a far higher transmittance in the visible region. The high density coating of nanorods showed a transmittance of visible light that was quite close to that of the coating of nano-hemispheres, while retaining a high shielding efficiency in near infrared region. More importantly however, the absorption peaks of the coating of nanorods lies at longer wavelengths than for the nano-hemispheres, which considerably improves the relatively indifferent performance [4] of gold nano-hemispheres in this application. This indicates that use of the nanorods would result in a higher efficiency in solar screening applications.

Ageing/annealing of rods

The structural instability of gold nanorods is a possible concern for some potential applications, with shape change and aging of the rods having been reported under various conditions [35, 37, 38]. It is clear that gold nanorods are thermodynamically unstable structures, not only because their surface-to-volume ratio can be readily reduced by spheroidization, but also because their flanks are comprised of the relatively unstable Au{110} and Au{100} crystal planes [13]. There is evidence that gold nanorods can melt at as low as 280°C [39], although other evidence puts the lower limit on the melting point at about 500 or 600°C [40, 41]. We considered therefore that there was a possibility that the rods might age during long service, even at ambient temperatures, with an attendant change in optical properties. This tendency to spheroidize was assessed by accelerated aging tests, in which the samples were annealed at temperatures ranging up to 240°C. Both low density and high density nanorod coatings are prepared for the aging test. The aspect ratio of gold nanorods in these coatings was 1.5 ~2.0. For the low density coatings, only a sub-monolayer of gold nanorods was deposited on the surface of the glass substrate, while in the case of the high density coatings, the stacked gold nanorods formed a cross-linked network.

In the case of the low density coatings, the absorption peak at about 540 nm became quite significant with an increased annealing temperature, while the broad peak at around 750 nm both diminished and blue-shifted during the annealing process (Figure 8). As mentioned previously, this latter peak is caused by the longitudinal plasmon resonance of the rods, while the former peak is due to both the

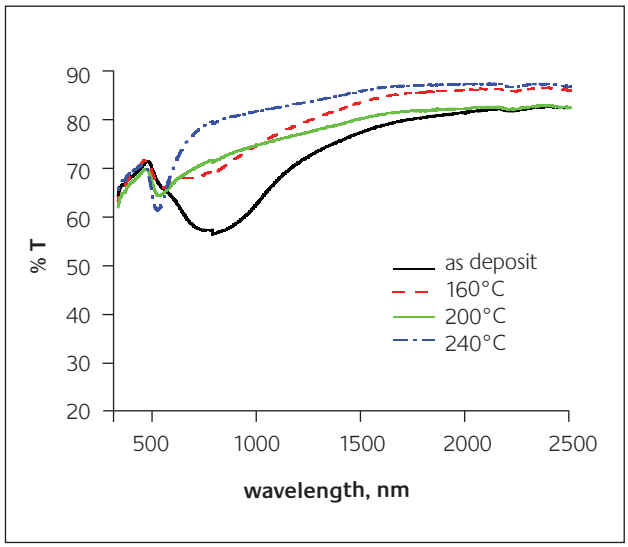

Figure 8
Transmittance of lower density coatings of gold nanorods during annealing

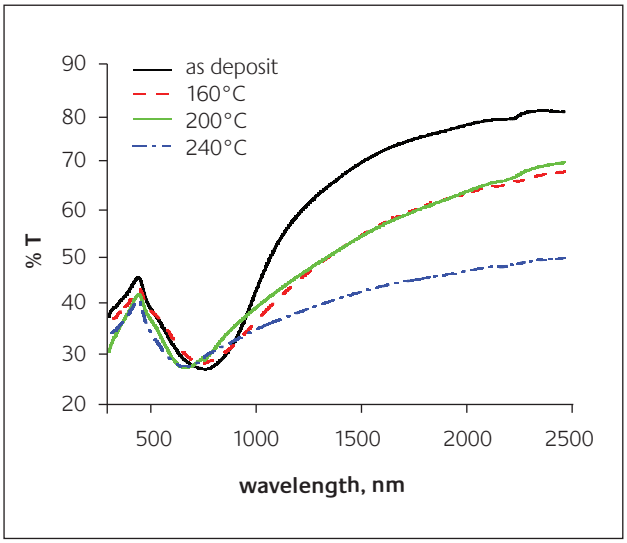

Figure 9

Influence of annealing on the transmittance of high density coatings of gold nanorods

transverse resonance of the rods and to the resonance of spheres. There was a concurrent evolution of the colour of the coating from blue to reddish as the annealing temperature was raised. In addition, absorption in the infrared region dropped slightly.

The optical transmission spectra of gold nanorod coatings of high packing density are shown in Figure 9. Here too there is a blue-shift in the main absorption peak as the particles are annealed. However, there is little evidence of a peak at 540 nm at any stage in the process. Furthermore, in contrast to the low density coatings, the overall transmittance of the coating in the infrared region decreased after annealing while that in the visible remained substantially unchanged. Note however the considerably lower overall transmittance of the high density coatings in comparison to the low density ones.

Typical SEM images showing the morphology of both low- and high-density coatings of gold nanorods during the accelerated aging process are given in Fig. 10. Annealing of the low density coating causes the separate nanorods to aggregate, grow in size, lose their rod shape, and change into irregular hemispheres (Figure 10(a1) to (a4)). There appear to be two stages during this process, at least when the aging was conducted at 200°C. First the rods contracted to spherical shapes, and only after this did the individual spheres coalesce to form larger irregular hemispherical shapes. The growth in size of individual particles in the high density coatings was not as obvious (Figure 10(b1)-(b4)) as in the low-density coatings. However, there is also evidently an evolution of shape during the annealing process, with the rods starting to coalesce into clusters of spheres or hemispheres.

An important issue is whether there are other processes taking place in the rods during annealing besides just shape change. In particular, the flanks of the rods are believed to be sheathed in a bi-layer of the CTAB surfactant, and this is likely to dissipate during aging or annealing. Thermogravimetric

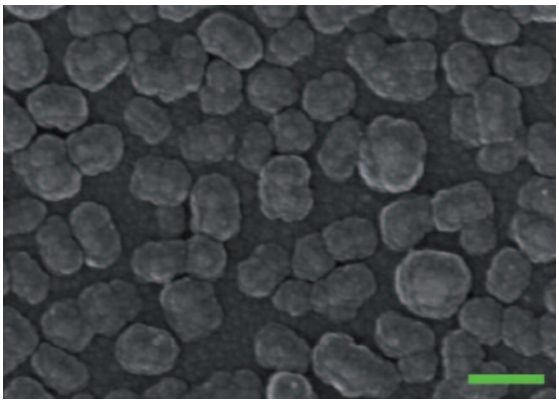

(a1) – as deposit

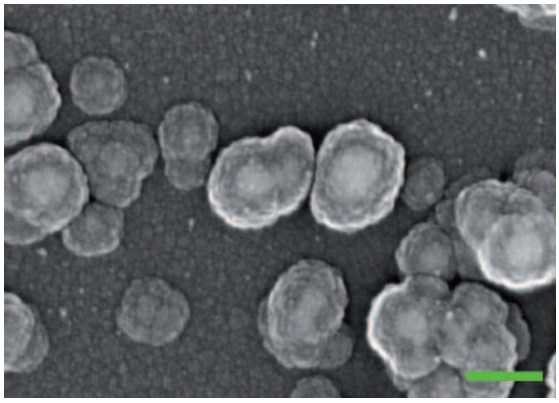

(a2) – 160°C, 5h

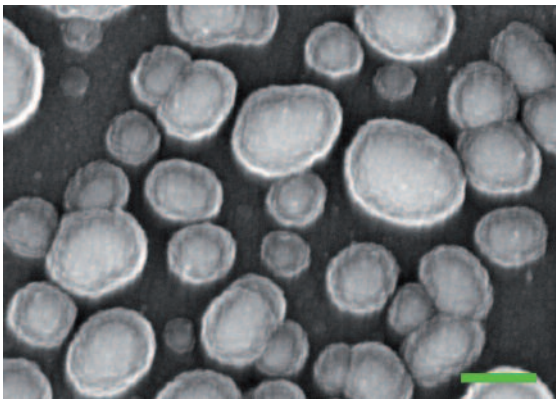

(a3) – 200°C, 3h

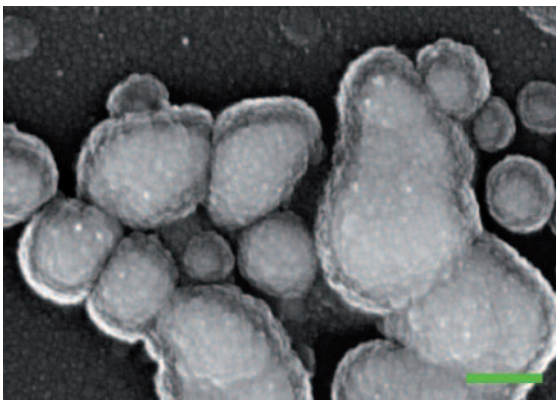

(a4) – 240°C, 1.5h

(a) low density gold nanorods coating

Figure 10

Evolution of the morphology of the coatings during accelerated aging. (green bars in SEM images indicate 100 nm)

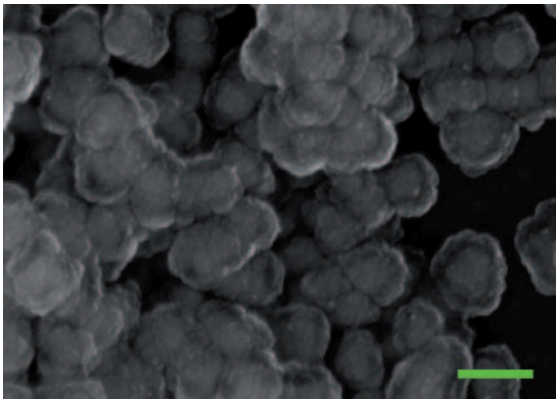

(b1) – as deposit

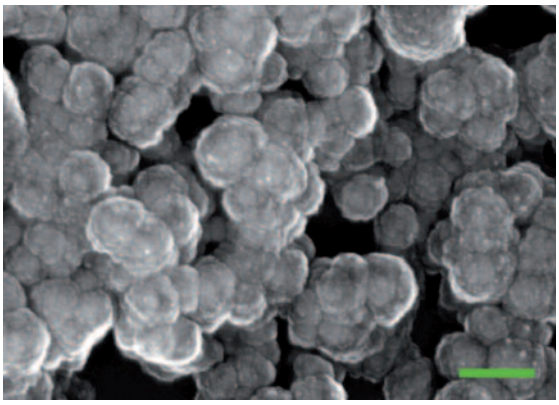

(b2) – 160°C, 5h

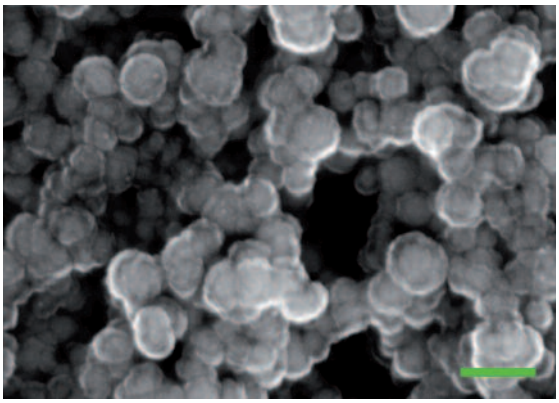

(b3) – 200°C, 3h

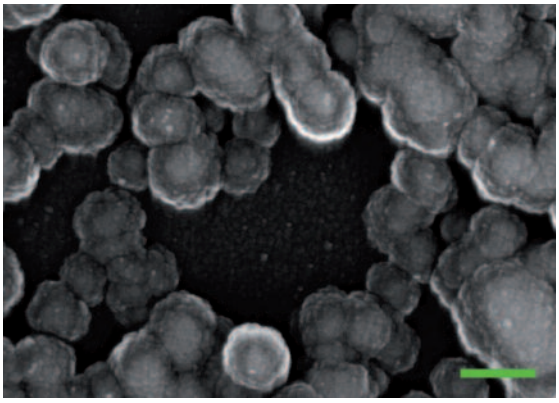

(b4) – 240°C, 1.5h

(b) high density gold nanorods coating

Figure 10

Evolution of the morphology of the coatings during accelerated aging. (green bars in SEM images indicate 100 nm)

analyses (TGA) of the purified gold nanorods (Figure 11) indicate that they are normally sheathed with about 20 %w/w of CTAB. The TGA results of pure CTAB crystals showed that they began to decompose and dissipate at 180°C with the process completely finished at 250°C, and a comparison between the two panels of Figure 11 indicates that this behaviour was mirrored with respect to the CTAB sheathing the gold nanorods. While present, the insulating CTAB layer inhibits movement of free electrons between nanoparticles and enhances the absorptive plasmonic response of the coating. However, annealing destroys the insulating layer and improves electrical conductivity in the network structure of the coating. This enhances reflection of infrared radiation [1]. Overall, the process has similarities with the growth of island metal films, which make a transition from absorptive to reflective behaviour as their connectivity and density is increased, even while remaining reasonably transparent in the visible [5].

Theoretical calculations illustrate neatly how spheroidization of the rods can shift the optical properties of these coatings (Figure 12). The aspect ratio of gold nanorods in this Figure are varied from 4 through to 1 (spheres) but their volume is kept constant. It is evident that there is a consequent blue shift and weakening of the extinction due

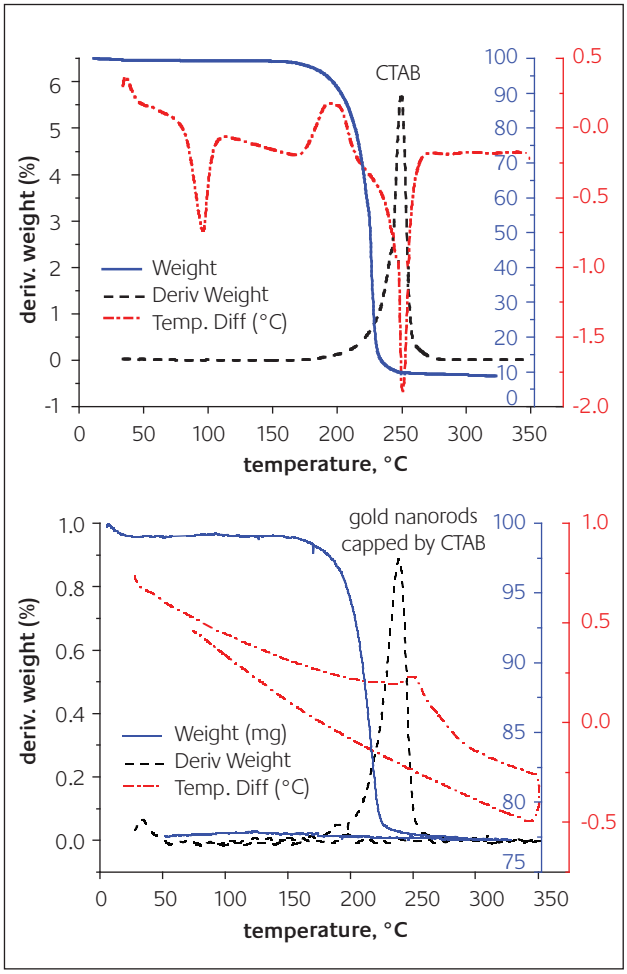

Figure 11

TGA result for CTAB and gold nanorods capped with CTAB, (a) pure CTAB, (b) gold nanorods capped with CTAB

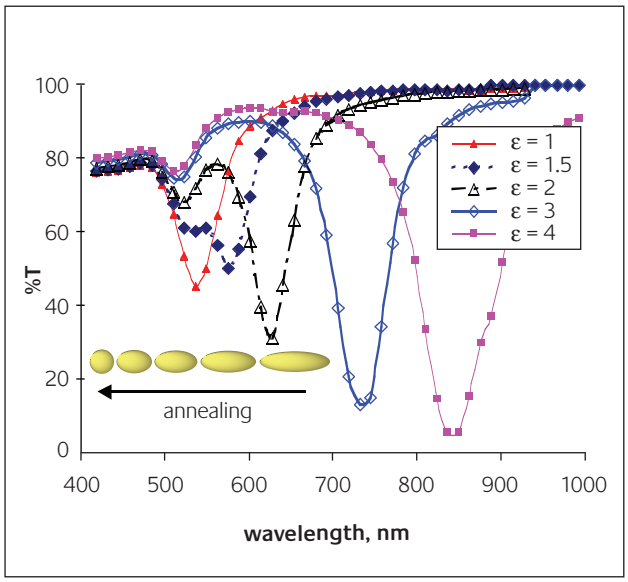

Figure 12
Simulation of evolution of optical transmission of a low density coating of gold nanorods during annealing

to the longitudinal plasmon resonance. However, the optical extinction at about 540 nm (due to the transverse plasmon resonance) is enhanced during the process.

Particle-particle interactions

Although the aspect ratio and density of coverage of the particles are important, if not dominant, factors in the determination of the optical properties of these coatings, there is a third factor that must be considered as well. This is the dipole-dipole interaction between adjacent gold nanoparticles that will cause a further absorption peak at around 700 nm [3, 8]. This effect is proportional to $(R/d)^{2L+1}$, where R is particle radius, d is the interparticle distance, and L is the multipole order (L=1 for dipole, L=2 for quadrupole, etc.) in the case of gold nanospheres [42]. Both increasing size and reducing spacing of particles will reinforce the effect. The effect of dipole-dipole interactions on adjacent spheres is illustrated in Figure 13. In Figure 13(a) we show the red shifting and broadening of the optical extinction peak that occurs when the size of a gold sphere is increased but the distance between the sphere centres is held constant. In Figure 13(b) we show the effect of fixing the sphere size but varying the distance between their centres. There is a weaker enhancement of the dipole-to-dipole interactions in this case.

Of course, the quantity of gold on the glass surface is fixed during the annealing process, so in practice the growth of nano-hemispheres must be associated with an increase in the particle-to-particle distance. In Figure 14 we show a simulation of this situation. Although larger particle size strengthens the absorption, the concurrent increase in interparticle distances reduces the contribution of the dipole-to-dipole interactions. While not shown here, it is also worth noting that the proportion of the light that is scattered rather than absorbed increases as the particle size increases. Scattering is less desirable than absorption in window

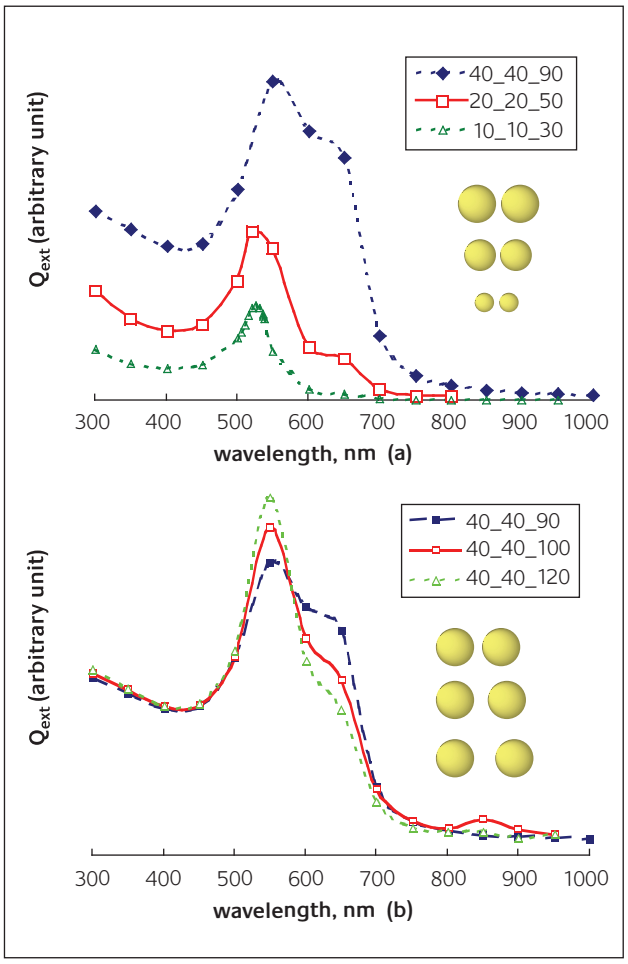

Figure 13
Simulation of the optical properties of closely spaced pairs of gold nanospheres. The notation used in the legend of this figure and the following one is s_t_u where s and t are the particle radii and u the distance between their centres. (a) Gap between particles kept constant at 10 nm, and (b) radii of particles kept constant at 40 nm and gap between them varied

coatings because it leads to a milky appearance. In general therefore, coarsening of particles is undesirable in this application. Overall, the optical properties of the coatings are based on the interplay between particle size, aspect ratio and spacing.

Discussion: Designing an ideal coating

As deposited, the low density coatings of gold nanorods inherited the optical properties of their parent colloids. Therefore, for coatings of this type, in which the individual nanoparticles behave as discrete entities, control of the spectral selectivity is mostly determined by the aqueous chemistry of the rod-growing solutions. Furthermore, we have shown that these coatings should be relatively resistant to thermally activated spheroidization under ambient conditions with temperatures of over 100°C required before changes occur.

The suitability of a coating for solar screening can be assessed by calculating the ratio of the proportion of visible

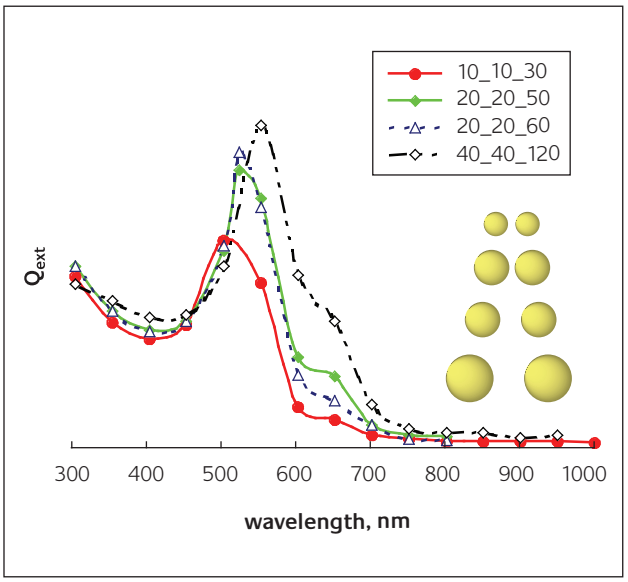

Figure 14

Simulation of the optical extinction of a coating of gold nanorods during the later annealing stages. Here particle size and gap both change simultaneously. The particle radii grow from 10 to 40 nm, while the gaps between them increase from 10 to 40 nm

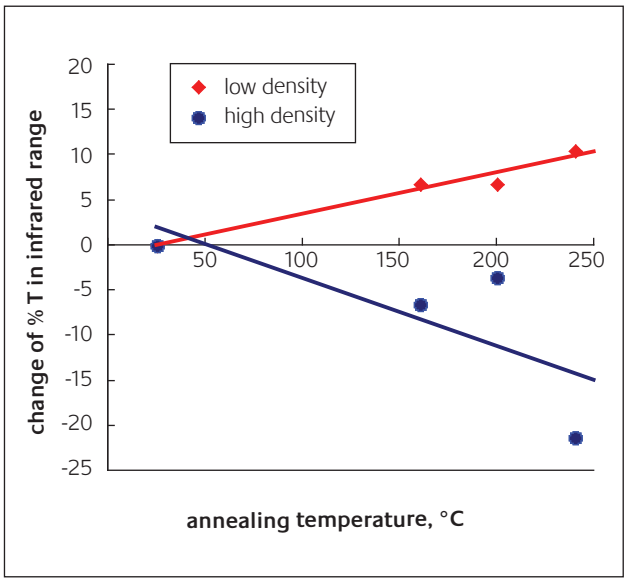

Figure 15

Change of transmittance in infrared range during annealing, determined by integration of the spectra between 700 and 2500 nm

light transmitted (T_{vis}) to total radiation received (T_{sol}). Theoretically, the maximum value of this ratio that can be obtained is 2.08 under standardized conditions [4]. Existing commercial solar screening products display values in the range 0.9 to 1.9 [4]. The solar control glass panes offered by Pilkington, for example, have values of T_{vis}/T_{sol} in the range 1.33 to 1.43. The as-deposited low density coating in the present work displayed a ratio of 1.0, which decreased (as expected) to 0.85 when the sample was annealed at 240°C. The ratio T_{vis}/T_{sol} for the high density coating was in the range 0.9-1.0 and was not much altered by annealing. The overall trend was that annealing decreased transmission of infrared wavelengths in the high density coating but increased it for the low density coating (Figure 15). Nevertheless these experimental coatings are, as they stand, not obviously commercially competitive yet.

The key to improving the spectral selectivity of these coatings will be to blend nanorods of varying aspect ratios in a controlled fashion. The simulated performance of an example of such a mixture, which notionally contains a blend of rods with aspect ratios spread between 3.0 and 10.0 and an effective radius [30] of 20 nm, is given in Figure 16. The assumption of well-separated gold nanorods was made in this simulation, *i.e.* the extinction effects are linearly additive, and dipole-to dipole interaction between the rods are negligible. This is reasonable as we have recently shown elsewhere [36] that the dipole-dipole interaction between rods is attenuated or even absent when they have sufficiently different aspect ratios. A coating containing this mixture would have T_{vis}/T_{sol} of 1.44 if applied at a gold loading of 0.26 g/m^2 of window, would transmit 52% on incident solar radiation falling on it (reduced to 45% once the absorption and reflection of the underlying glass [4] is taken into account), and would have a pale pink colour in transmission.

There are four regions of interest, marked A to D, in Figure 16. The absorption peak at A is due to the plasmon resonances at about 530 nm and cannot be avoided in unpolarised light. The broad transmission peak at B would cause a pink hue in the coatings, but would be reduced by particle-to-particle interactions. (These have not been taken into account here). The broad absorption trough marked C is responsible for the spectral selectivity. If reliable large-scale production of rods with aspect ratios greater than 10.0 could be achieved, then the width of the trough could potentially be extended into the infra red of region D. At a gold loading of, for example, 0.26 g Au/m^2 and a gold price of $450 per troy ounce, this coating would contain US$3.76/m^2 which is competitive in cost with commercial products of similar performance. Current state-of-the art commercial solar films with retail for in excess of US$100/m^2 while even plain

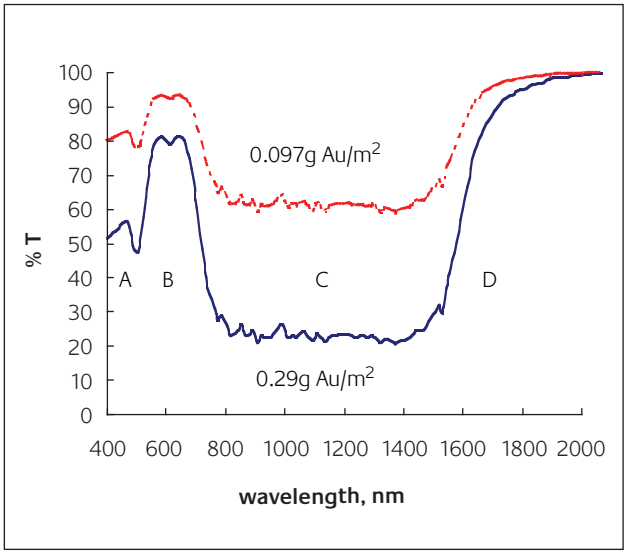

Figure 16

Simulated transmission spectra of hypothetical mixtures of gold nanorods with aspect ratios spread between 3 and 10

window glass retails at about US$30/m^2 upwards in many countries. Therefore, it seems to us entirely feasible that a gold-based coating could compete provided that it could be cheaply manufactured and applied.

Conclusions

The unique optical properties of gold nanorods, which exhibit tuneable absorption as a function of their aspect ratio, suggest that they may have potential applications in coatings for solar control on windows. Here we have explored the properties of coatings produced by attaching gold nanorods to the surface of glass. Such coatings can attenuate solar radiation effectively, even at very low gold contents. However, the figure-of-merit, T_{vis}/T_{sol}, of our experimental coatings was close to unity, indicating that their attenuation is not sufficiently spectrally selective. However, we show, in theory anyway, how a blend of rods with aspect ratios between 3.0 and 10.0 can produce a coating with T_{vis}/T_{sol} of ~1.4. If rods with aspect ratios greater than 10.0 could be reliably produced in quantity, then the figure-of-merit of these coatings could theoretically be improved further.

Acknowledgements

The authors thank Dr Richard Wuhrer for assistance with scanning electron microscopy. This work has been supported by the Australian Research Council (LP0560475) and by resources and mining company AngloGold Ashanti.

References

1 N. Kaiser and H.K. Pulker, in *Optical Interference Coatings*, Springer, 2003
2 T.E. Johnson, in *Low-e Glazing Design Guide*, Butterworth Architecture, 1991
3 X. Xu, M. Stevens and M.B. Cortie, *Chem. Mater.*, 2004, **16**, 2259
4 H. Chowdhury, X. Xu, P. Huynh and M.B. Cortie, *ASME Journal of Solar Energy Engineering*, 2005, **127**, 70
5 X. Xu, M.B. Cortie and M. Stevens, *Mater. Chem. Phys.*, 2005, **94**, 266
6 M. Quinten, *J. Cluster Sci.*, 1999, **10**, 321
7 C.J. Murphy, T.K. Sau, A.M. Gole, C.J. Orendorff, J. Gao, L. Gou, S.E. Hunyadi and T. Li, *J. Phys. Chem. B*, 2005, **109**, 13857
8 K.E. Peceros, X. Xu, S.R. Bulcock and M.B. Cortie, *J. Phys. Chem. B*, 2005, **109**, 21516
9 J. Liu, A.I. Maaroof, L. Wieczorek and M.B. Cortie, *Adv. Mater.*, 2005, **17**, 1276
10 K.L. Kelly, E. Coronado, L.L. Zhao and G.C. Schatz, *J. Phys. Chem. B*, 2003, **107**, 668
11 Y.-Y. Yu, S.-S. Chang, C.-L. Lee and C.R.C. Wang, *J. Phys. Chem. B*, 1997, **101**, 6661
12 X. Xu and M.B. Cortie, *Adv. Func. Mater.*, 2006, in press
13 J. Perez-Juste, I. Pastoriza-Santos, L.M. Liz-Marzan and P. Mulvaney, *Coordin. Chem. Rev.*, 2005, **249**, 1870
14 C.G. Blatchford, J.R. Campbell and J.A. Creighton, *Surf. Sci.*, 1982, **120**, 435
15 B. Nikoobakht and M.A. El-Sayed, *J. Phys. Chem. A*, 2003, **107**, 3372
16 N. Taub, O. Krichevski and G. Markovich, *J. Phys. Chem. B*, 2003, **107**, 11579
17 Z. Wei and F.P. Zamborini, *Langmuir*, 2004, **20**, 11301
18 Z. Wei, A.J. Mieszawska and F.P. Zamborini, *Langmuir*, 2004, **20**, 4322
19 S. Hsieh, S. Meltzer, C.R.C. Wang, A.A.G. Requicha, M.E. Thompson and B.E. Koel, *J. Phys. Chem. B*, 2002, **106**, 231
20 O.-H. Kwon, S. Lee and D.-J. Janga, *Eur. Phys. J. D*, 2005, **34**, 243
21 E. Dujardin, L.-B. Hsin, C.R.C. Wang and S. Mann, *Chem. Comm.*, 2001, 1264
22 J.K.N. Mbindyo, B.D. Reiss, B.R. Martin, C.D. Keating, M.J. Natan and T.E. Mallouk, *Adv. Mater.*, 2001, **13**, 249
23 Y. Niidome, H. Takahashi, S. Urakawa and E. Al, *Chemistry Letters*, 2004, **33**, 454
24 K.G. Thomas, S. Barazzouk, B.I. Ipe, S.T.S. Joseph and P.V. Kamat, *J. Phys. Chem. B*, 2004, **108**, 13066
25 A. Gole, C.J. Orendorff and C.J. Murphy, *Langmuir*, 2004, **20**, 7117
26 C.J. Orendorff, P.L. Hankins and C.J. Murphy, *Langmuir*, 2005, **21**, 2022
27 A. Gole and C.J. Murphy, *Chem. Mater.*, 2005, **17**, 1325
28 B. Nikoobakht and M.A. El-Sayed, *Chem. Mater.*, 2003, **15**, 1957
29 N.R. Jana, L.A. Gearheart and C.J. Murphy, *J. Phys. Chem. B*, 2001, **105**, 4065
30 B.T. Draine and P.J. Flatau, User Guide to the Discrete Dipole Approximation Code DDSCAT 6.1, 2004
31 B.T. Draine and P.J. Flatau, *J. Opt. Soc. Am. A*, 1994, **11**, 1491
32 C.F. Bohren and D.R. Huffman, in *Absorption and Scattering of Light by Small Particles*, Wiley, 1998
33 B.T. Draine, *http://arxiv.org/abs/astro-ph/0309069*, 2003
34 J.H. Weaver and H.P.R. Frederikse, Optical Properties of Selected Elements. In D.R. Lide (Ed.), *CRC Handbook of Chemistry and Physics*, CRC Press, Boca Raton, 2001, pp. 12-133
35 D.A. Zweifel and A. Wei, *Chem. Mater.*, 2005, **17**, 4256
36 M.B. Cortie, X. Xu and M.J. Ford, *Physical Chemistry : Chemical Physics*, 2006, **8**, 3520
37 Z.L. Wang, R.P. Gao, B. Nikoobakht and M.A. El-Sayed, *J. Phys. Chem. B*, 2000, **104**, 5417
38 L. Gou and C.J. Murphy, *Chem. Mater.*, 2005, **17**, 3668
39 C.-H. Chou, C.-D. Chen and C.R.C. Wang, *J. Phys. Chem. B*, 2005, **109**, 11135
40 A.-S.A.-M. Al-Sherbini, *Colloids and Surfaces A: Physicochem. Eng. Aspects*, 2004, **246**, 61
41 M.B. Cortie, *Gold Bull.*, 2004, **37**, 12
42 Z. Liu, H. Li, X. Feng, S. Ren, H. Wang, Z. Liu and B. Lu, *J. Applied Phys.*, 1998, **84**, 1913